CHAPTER VII
ANIONIC SURFACTANTS INTERCALATED LAYERED DOUBLE HYDROXIDES BASED-LOW DENSITY POLYETHYLENE NANOCOMPOSITES

7.1 Abstract

Low density polyethylene/layered double hydroxide (LDH) nanocomposites were prepared via melt-compounding using polyethylene grafted maleic anhydride (PE-g-MAH) as a compatibilizer. The pristine LDH-CO_3 was first converted to LDH-NO_3 for facilitating the intercalation process of polyethylene chains. LDH-NO_3 was modified by different alkyl chain length of sodium sulfates (n_c = 8, 12, and 20) using ion exchange method. The successful intercalation of the anionic surfactants into LDH layers was characterized by X-ray diffraction (XRD), Fourier transform infrared (FTIR), scanning electron microscopy (SEM), and thermogravimetry (TGA). It was observed that the size of the anionic surfactants played a vital role for the difference in morphological and thermal properties. The obtained nanocomposites established partially exfoliated/intercalated mixed morphology. The degree of exfoliation and intercalation depends not only on the chain length of the anionic modifiers used but also the interactions between the alkyl chains of anionic modifiers and the LDH layers. Either exfoliated or highly intercalated structure was preferable when the number of alkyl chain length is larger ($\geq$ 12). The TGA results of LDPE/organomodified LDHs composites exhibited remarkable improvement of the thermal properties, i.e. the decomposition temperature was 20–33 ^{o}C higher than the pure matrix. The DSC results showed slight increase of crystallization temperature, while no significant change for both melting and degree of crystallinity were observed. Both storage modulus and relative glass transition (β relaxation) temperature for the nanocomposites was enhanced by the addition of organomodified LDHs and more noticeable for the composite containing LDH-C8. With increasing the concentration of the organomodified clay, the thermal properties and the storage modulus were significant enhanced, but the large aggregated-LDH platelets were observed.

(**Key-words**: organomodified LDHs, anionic surfactants, morphological feature, LDPE nanocomposites, melt intercalation)

7.2 Introduction

Layered double hydroxides (LDHs), commonly known as hydrotalcite-like compounds or anionic clays, are a class of host-guest materials, which the general formula $[M^{2+}_{1-x}M^{3+}_{x}(OH)_2]^{x+}A^{n-}_{x/n}mH_2O$, where M^{2+} is divalent metal ions (i.e. Mg^{2+}, Zn^{2+}, etc.), M^{3+} is trivalent metal ions (i.e. Al^{3+}, Cr^{3+}, etc.), A is an anion with valency n (i.e. CO_3^{2-}, Cl^-, NO_3^-, etc.) or organic anion, m is the number of interlayer water, and x determines the layer charge density and anion exchange capacity with generally range between 0.2 to 0.4 (Brown, 1967; Miyata, 1973; Cavani, 1991). These materials are structurally similar to the mineral brucite ($Mg(OH)_2$), in which a partial M^{2+} ions replaced by M^{3+} ions, such replacement results in a net positive charge on the octahedral layers. This excess charge is balanced by the anions located in the interlayer region where the hydration water molecules also accommodated (Cavani, 1991 and Reichle, 1986).

Owing to their highly tunable and unique anion exchange properties, LDHs are being considered as new emerging layered host materials that can be tailored to accommodate a wide range of guest molecules to create novel solids with desirable physical and chemical properties controlled by host-guest and guest-guest interactions (Auerbach *et al.* 2004). As a layered host, LDHs have been used for many potential applications like catalysts, ceramic precursors, ion exchangers, absorbents, medicine stabilizers, and controlled release of anions (Constantino, 1995; Arco, 1999; Xu, 1998; Hermosin, 1996; Qian, 1997; Ambrogi, 2001). Very recently, their potential as nanofiller for preparing polymer nanocomposites has been received considerable attention from both academia and industrial points of view. In contrast to the conventional layered silicates (i.e. MMT), layered double hydroxides (LDHs) possess certain inherent advantages, for example, being mostly synthetic origin and a wide range of chemical composition can be obtained by changing the type and molar ratio of the metal ion pairs during the synthesis. In addition, the unique positive

charge of LDHs crystal layers provides a greater flexibility in selecting the suitable organic modifiers. However due to their strong interlayer electrostatic interactions and small gallery space (~0.76 nm), which is not only suitable for the penetration of the long polymer chains into the interlayer region but also the hydrophilic nature of LDH layers makes them incompatible with hydrophobic polymers. For this sense, it is necessary to pay attention on the importance of the chemistry used to modify their surface, in order to minimize the attractive force between such layers, and to achieve a good dispersion and good exfoliation of LDH layers in matrix polymer. The layered LDH should be modified with a suitable, usually organic-anions with intention of increasing both interlayer distance and hydrophobicity of LDH layers, known as organomodified LDHs (Crepaldi *et al.* 2000).

There are several ways reported in literatures for preparing organomodified LDHs, i.e. anion-exchange of a precursor LDH, direct synthesis by coprecipitation, regeneration method, and thermal reaction. Since the carbonate anion is readily accommodated and tenaciously held in the interlayer, carbonate contamination was usually observed for all methods. The anion-exchange method has been found to be the most common method for preparation organomodified LDHs. Several anionic species such as phosphates, carboxylates, sulfonates, and sulfates have been widely used to modify the layered LDH via this process (Newman and Jones, 1998). In particular, alkyl sulfates have been found to be the most efficient classes of the anionic surfactants for LDH modification. The exchange reaction is controlled by the selectivity of the layered host for the different anions. The previous study by Miyata *et al.* (1983) has demonstrated the selectivity scale of exchangeable anions as following: $CO_3^{2-} > SO_4^{2-} >> OH^- > F^- > Cl^- > Br^- > NO_3^- > ClO_4^-$. The LDH containing ClO_4^-, NO_3^- or even Cl^- have been considered as suitable precursors for uptaking long-chain organic anions since they are large anion-exchanging capacity.

So far, LDH based polymer nanocomposites have been extensively investigated with a large number of polymers, including, epoxy (Hsueh and Chen, 2003), polyamide (Hsueh and Chen, 2003), poly(ethylene terepthalate) (PET) (Lee *et al.* 2006), poly(vinyl alcohol) (PVA) (Messersmith and Stupp, 1995), poly(ε-carprolactone) (Costatino and Vittoria, 2009), polypropylene (Ding, 2006;

Kuppinger, 2007; Coiai, 2009) and polyethylene (Chen, (2003 and 2004); Qiu, 2006; Costa, (2005, 2006, 2007); Du, 2006; Costantino, 2005) etc. Among these polymers, polyethylene (PE) is one of the fastest growing classes of thermoplastics due to its good balance of favorable processability, mechanical properties, and chemical resistance, which has been extensively used in both packaging and engineering applications. The considerable research efforts have been made on LDH based polyethylene nanocomposites mainly focusing on solution intercalation process; details of individual work have been well documented in the literature (Chen, 2003 and 2004; Qiu, 2006). However, not much work has been reported on melt intercalation technique for preparing polyethylene/LDH nanocomposites (Costa, (2005, 2006, 2007); Du, 2006; Costantino, 2005) for examples, Costa *et al.* (2005) first reported the preparation of intercalated/flocculated LDPE/SDBS-LDH nanocomposites using melt intercalation process. A complex morphological feature of dispersed LDH particles was observed with mostly located in the form of thin platelets and agglomerates. The rheological studies i.e. dynamic frequency sweep experiments were performed to explain the nature of the dispersed LDH particles. A significant changes in linear viscoelastic responses in low frequency region was observed i.e. storage modulus (G') of the composites was higher than pure LDPE even at very low loading (2 phr) of SDBS-LDH. They suggested this behaviour was related to the formation of network-like structure via the interaction between LDHs particles and polymer chains. Although, the morphological analysis by XRD and TEM of such composites did not evidence a homogeneous dispersion and a perfect exfoliation of LDH particles, the thermal stability and fire resistant properties of these composites were significantly enhanced (Costa *et al.* 2007), which could be ascribed to the barrier effect of LDH layers on the oxygen diffusion that can shield PE chain segments from thermal oxidation. This result was similar to the case of LLDPE/DS-LDH nanocomposites (Du and Qu, 2006) and PE/stearate-LDH nanocomposites (Costantino *et al.* 2005). Though, organic modification of LDHs seems to be enough for the preparation of nanocomposites based on PE, but the use of the third component, named compatibilizer which is a functionalized polymer containing pendent maleic anhydride group on polyethylene backbone (PE-g-MAH), is very necessary to improve the degree of exfoliation of the composite. This is due

to the fact that the polar character of the anhydride can have favourable interaction with clay surface. Costa *et al.* (2006) has investigated how chemical compatibility of the polymer matrix influenced on morphological and rheological properties of composites using two different types of PE matrices: one with unmodified PE and the other with PE-g-MAH. SEM analysis evidenced that the single platelets remained more intensely coated by polymer in MAH grafted PE system, while they trended to form structural association or clusters for the unmodified PE system. This result was supported by the larger increase in the storage modulus in the more polar polymer system, which came from the differences in polymer–particle and particle–particle interactions that the matrix polarity favored the dispersion of LDH particles.

In this study, the pristine LDH-CO_3 was first converted to LDH-NO_3 for facilitating the intercalation process of PE chains, we reported the synthesis and characterizations of LDH-NO_3 by anion exchange method with alkyl sulfate anionic surfactants having different alkyl chain lengths (n_c = 8, 12, and 20, Figure 7.1). The evidences of anionic surfactants intercalated layered LDH on morphological and thermal properties were studied by X-ray diffraction (XRD), Fourier transform infrared (FTIR), scanning electron microscopy (SEM), and thermogravimetry (TGA) to understand the role of anionic surfactants. The LDPE nanocomposites with those organo-LDHs were prepared by melt intercalation process. The morphological and thermal properties of the nanocomposites were also studied in order to evaluate the effect of LDHs dispersion in polymer matrix on their properties. The dynamic mechanical properties of nanocomposites were determined and discussed to study the effect of polymer chains confinement on their glass transition temperature (T_g).

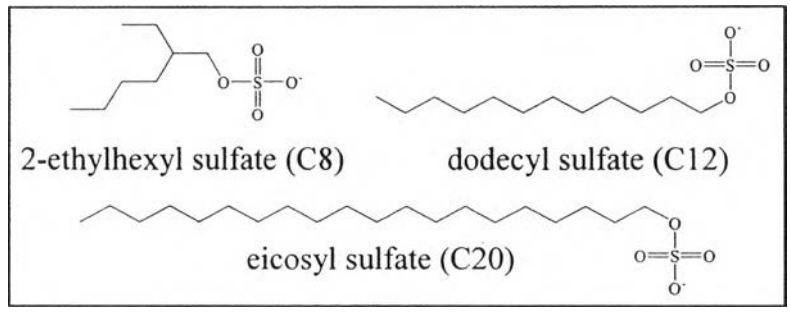

Figure 7.1 Chemical structures of anionic surfactants guest molecules used for intercalation LDH-NO_3.

7.3 Results and Discussion

7.3.1 Synthesis and Characterization of LDH-NO_3

It is well known that the CO_3^{2-} anions are strongly held in the interlayer region and that is very difficult to replace them with other anions using simple ions-exchange procedure. To increase the interlayer distance for facilitating long alky chain molecules, the CO_3^{2-} form (LDH-CO_3) was converted to NO_3^- form (LDH-NO_3) following the method as described by Miyata *et al.* (1983). As can be seen from XRD pattern (Figure 7.2(a)), LDH-NO_3 evidences a shift of the (003) basal peak from 2θ = 11.7 to 9.9°, corresponding to an enlargement of the basal spacing (d_{003}) from 0.76 to 0.89 nm. This increase is due to the replacement of monovalent NO_3^- ions that occupied a space corresponding to three oxygens, which is greater than that of occupied by other anions such as Cl^- and Br^-. The repulsion between NO_3^- ions led to the new orientation of N–O bond, which no longer parallel to the LDH layers, resulting an increase of interlayer distance. In addition, the diffraction peak at 2θ=11.5° related with the interlayer CO_3^{2-} anions disappears, suggesting the completely exchanged CO_3^{2-} by NO_3^- anions.

The successfully exchange of NO_3^- anions was confirmed by FTIR analysis as shown in Figure 7.2(b). The LDH-NO_3 shows a characteristic peaks at 1384 and 839 cm^{-1} that can be attributed to the ν_3 and ν_2 vibration modes of NO_3^-, respectively. The adsorption peaks around 670 and 550 cm^{-1} can be attributed to the Al–OH and Mg–OH translation modes, respectively. The broad adsorption peak around 3459 cm^{-1} can be assigned to the –OH stretching, which owing to the presence of hydroxyl groups of LDH, cointercalated water molecules, or both (Velu *et al.* 1997). Similar FTIR result for LDH-NO_3 has also been reported by Tammaro *et al.* (2005).

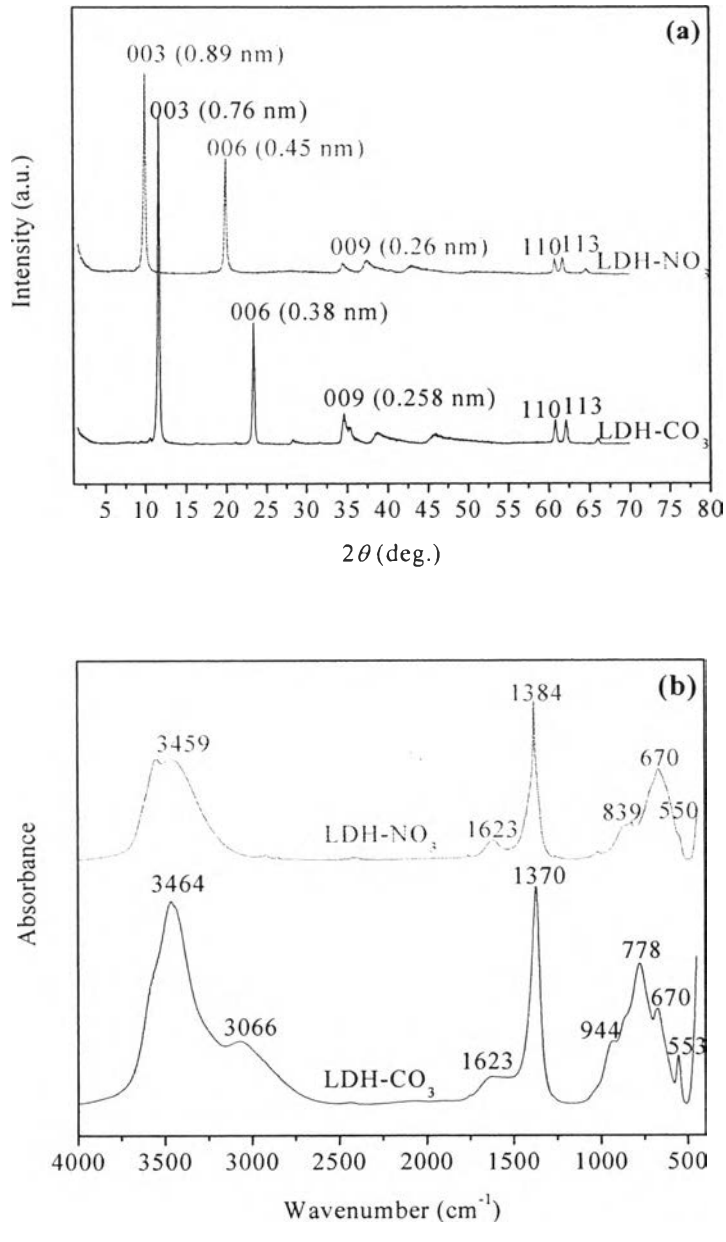

Figure 7.2 XRD patterns (a) and FTIR spectrum (b) of LDH-NO_3 as compared with LDH-CO_3.

7.3.2 Synthesis and Characterization of Organomodified LDHs

Figure 7.3(a) shows the XRD patterns of organomodified LDHs with different alkyl chain length of anionic surfactants. As can be seen, all samples evidence a significant shift of the (003) basal peak toward lower angles as increasing alkyl chain length (n_c), which consistent with an enlargement of d_{003} from 0.89 to 2.12, 2.42, and 3.25 nm when number of alkyl chain length (n_c) = 8, 12, and 20,

respectively (Table 7.1). Moreover, it was observed that XRD pattern of all organomodified LDHs shows a higher order reflections (00*l*) series with a sharp peaks (i.e. <006>, <009>), which demonstrates the formation of a well-ordered guest intercalated LDH layers. Although the modification process was carried out under nitrogen atmosphere to prevent carbonate contamination, a weak peak at $2\theta \cong 11.5°$ related to the cointercalation of carbonate anions, still exists for all samples.

The increase of the d_{003} of organomodified LDHs is a linear relation with the alkyl chain length (n_c) of the surfactants used, as shown in Figure 7.3(b). Similar observation was reported on both alkyl sulfate and carboxylate by Meyn *et al.* (1990 and 1993), suggested the monolayer arrangement of the surfactants and very recently in the case of alkyl sulfonate, suggested both mono and bilayer arrangement (Costa *et al.* 2008). It is well known that Meyn *et al.* (1990) has been made the theoretical calculations of the interlayer distance for various LDHs and surfactants. Regarding to those calculations, the monolayer arrangement was used in our case to evaluate how arrangement of the anionic surfactants, as in the following equation:

$$d_L = 0.96 + 0.127 * n_c * \sin\alpha \qquad (1)$$

where d_L (nm) is the d-spacing, n_c is the number of carbon atom in the alkyl chain of the surfactants, and α is the tilt angle of the alkyl from the normal of the metal hydroxide sheet. In the case of alkyl sulfate modified LDH, the value of tilt angle has been found to be 56° for the dried samples. In fact for the case organomodified LDHs that do not dried in vacuum, there exists the monolayer of water molecules in between the hydrocarbon chain end of the surfactant and the metal hydroxide layers (Meyn, 1990 and Carlino, 1997). Loss of this monolayer causes a contraction of interlayer spacing by 0.3–0.5 nm. It was found that the interlayer spacing of LDH modified with alkyl sulfate surfactants was decreased by 0.32 nm due to the loss of such monolayer water molecules. This value has been used for correcting the d-spacing calculated from equation (1). The corrected values are compared with the experimentally observed values as presented in Figure 7.3(b). Good agreement

between these two values, especially in the case of LDH modified with shorter alkyl chains length (LDH-C8 and LDH-C12), was evident. However for the longer one (LDH-C20), a small difference was observed that presumably due to the difference in the tilt angle (Carlino, 1997). Therefore, it can be postulated in our case that these alkyl sulfate surfactants oriented between the LDH layers in the monolayer fashion with the tilt angle about 56°.

The average crystallite size of LDH-NO_3 and organomodified LDHs is also calculated by using Scherrer equation:

$$L = (K \cdot \lambda)/(B \cdot \cos\theta) \qquad (2)$$

where, L (nm) is the crystallite thickness in the direction perpendicular to the plane of metal hydroxide sheet in LDH materials, λ is the wavelength of the radiation CuKα (0.15406 nm), K is the shape factor (0.9), B is the full-width at half-maxima (FWHM, rad.) and θ is Bragg diffraction angle (°). However, the width due to the machine brodening has not been corrected, thus the values obtained according to the Scherrer equation are an estimate value of the actual crystal thickness. Figure 7.3(c) shows that the estimate crystal thickness of the organomodified LDHs distinctly decreases as compared to the LDH-NO_3. With increasing alkyl chain length (n_c), the estimate crystal thickness of the organomodified LDHs tends to increase. Moreover. the average number of metal hydroxide layers (calculated from the ratio of the estimate crystal thickness and the d-spacing) of the organomodified LDHs is much smaller than that of LDH-NO_3 and not a linear relation with n_c like the case of d-spacing and the estimate crystal thickness (Figure 7.3(c)).

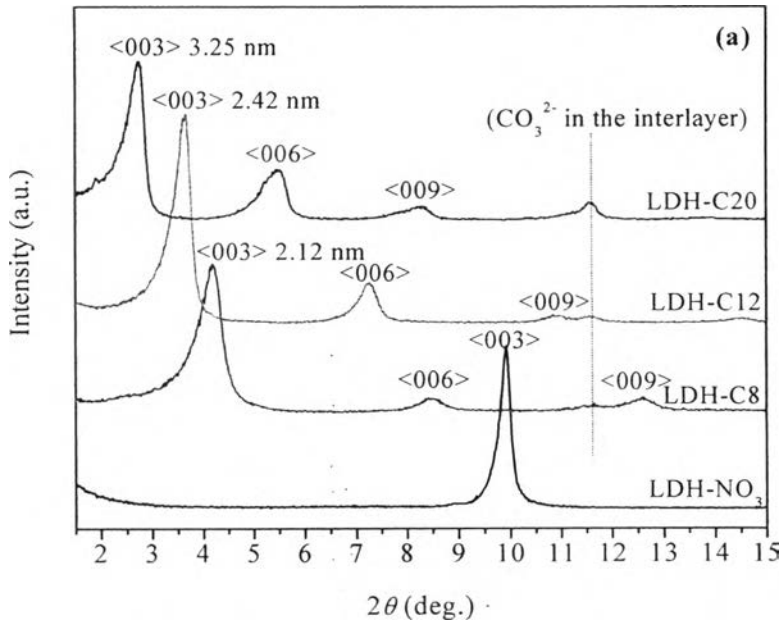
(a)
<003> 3.25 nm
<003> 2.42 nm
(CO3 2- in the interlayer)
<006>
<009>
LDH-C20
<003> 2.12 nm
<006>
<009>
LDH-C12
<003>
<006>
<009>
LDH-C8
LDH-NO3
Intensity (a.u.)
2θ (deg.)

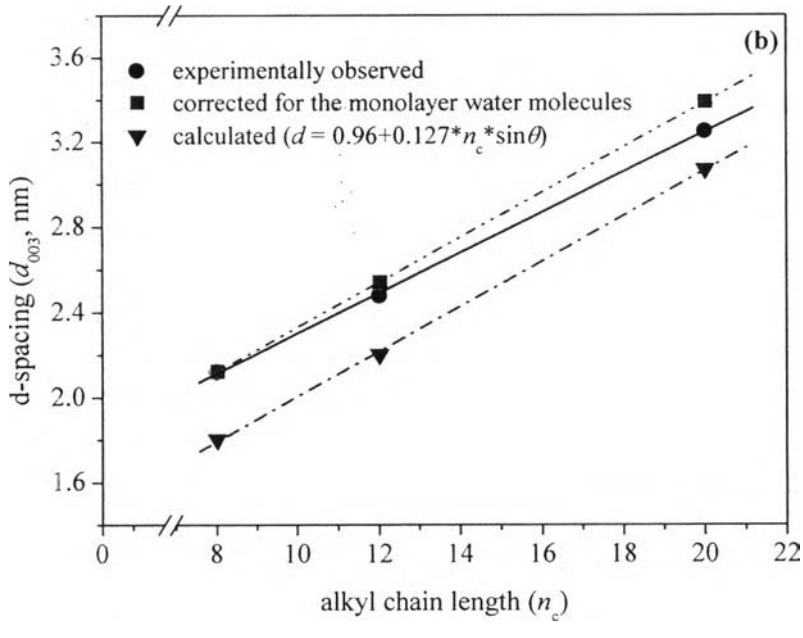
(b)
experimentally observed
corrected for the monolayer water molecules
calculated (d = 0.96+0.127*nc*sinθ)
d-spacing (d003, nm)
alkyl chain length (nc)

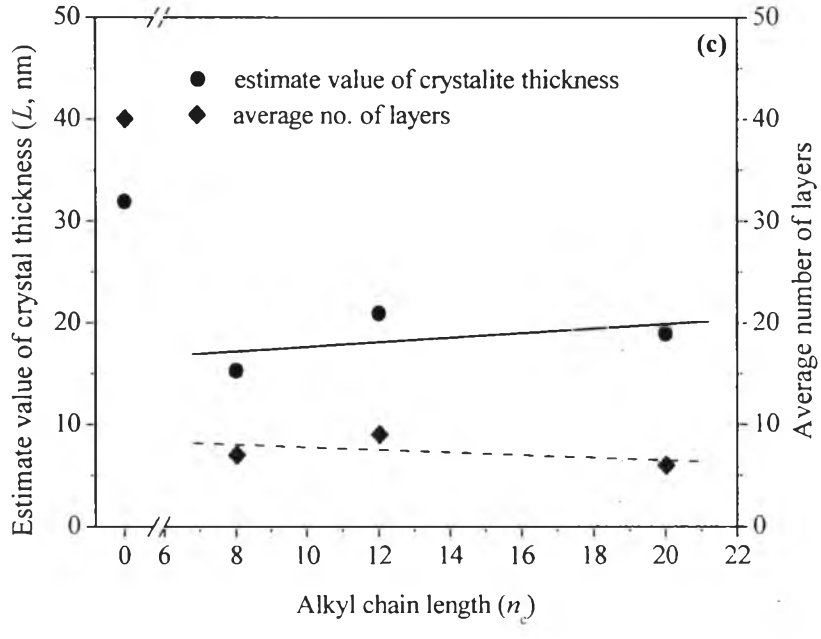

Figure 7.3 The effect of alkyl chain length (n_c) of sulfate surfactants on: (a) XRD pattern of the organomodified LDHs, (b) d-spacing and their arrangement between the LDH layers, and (c) estimate value of cystal thickness

Table 7.1 The reflections in <*00l*> series and interlayer spacing for LDH-NO_3 and the organomodified LDH with different alkyl sulfate surfactants

Sample	Alkyl chain length (n_c)	reflections in <*00l*> series (deg.)/ d-spacing (nm)			Arrangement in the interlayer LDH
		<003>	<006>	<009>	
LDH-CO_3	-	9.91 (0.89)	23.40 (0.38)	34.62 (0.26)	-
LDH-NO_3	-	9.91 (0.89)	19.88 (0.45)	34.62 (0.26)	-
LDH-C8	8	4.16 (2.12)	8.46 (1.04)	12.55 (0.74)	monolayer
LDH-C12	12	3.55 (2.42)	7.25 (1.22)	10.85 (0.81)	monolayer
LDH-C20	20	2.72 (3.25)	5.49 (1.61)	8.27 (1.07)	monolayer

The morphological features of pristine LDHs and the organomodified LDHs are presented in Figure 7.4(a)–7.4(e). High magnification SEM micrograph of the LDH-CO_3 (Figure 7.4(a)) reveals a stacking of hexagonal plate-like particles. The lateral dimension varies from 100–200 nm whereas the thickness is less than hundred nm. The highly anisometric nature of these particles is also evident. After it was exchanged by NO_3^- ions, the particle morphology seems to be unchanged (Figure 7.4 (b)). The hexagonal plate-like geometry still exists, only the particle thickness is increased (about 100–200 nm), which confirms the replacement of CO_3^{2-} anions by NO_3^- anions as consistent with the XRD and FTIR results. As a result, the particle with the thickness of about 200 nm and the d-spacing of 0.89 nm may contain around 225 metal hydroxide sheets (Lagaly and Beneke, 1991). Since the organic modification has been made, the changes of particle morphology were evident with respect to the size of alkyl sulfate surfactants (n_c) used. For the smallest one (n_c = 8, Figure 7.4(c)), the well-stacked of plate-like particles is lost. In stead they appear in aggregated form (see the inserted picture) with larger in size (~500 nm) and more roughness of surface than the pristine one. This irregular particle morphology might come from the ethyl branched of this surfactant hindered the ordering of the LDH layers. When the n_c was increased to 12 (Figure 7.4(d)), the well-stacked of hexagonal particles turn back appearance. It is more likely that these stacks tend to connect each others probably via the hydrophobic interaction as formerly reported (Lagaly and Beneke, 1991). Figure 7.4(e) shows the SEM images when the n_c equals to 20, it seems that the particle morphology is somewhat changed as compared to the others. In fact, the LDH-C20 particles arrange themselves in the nonuniform stacking of irregular hexagonal plate-like particles. Also, it appears uneven surface and unsharped edges, which probably came from the excess of anionic surfactants draped over the outer particles surface (Lagaly, 1991 and Pavan, 1999). As a result, it is clear that the size of the anionic surfactants played a vital role for the change of particles morphology and loss of crystallinity as previously reported for the case of using regeneration process (Costa *et al.* 2008).

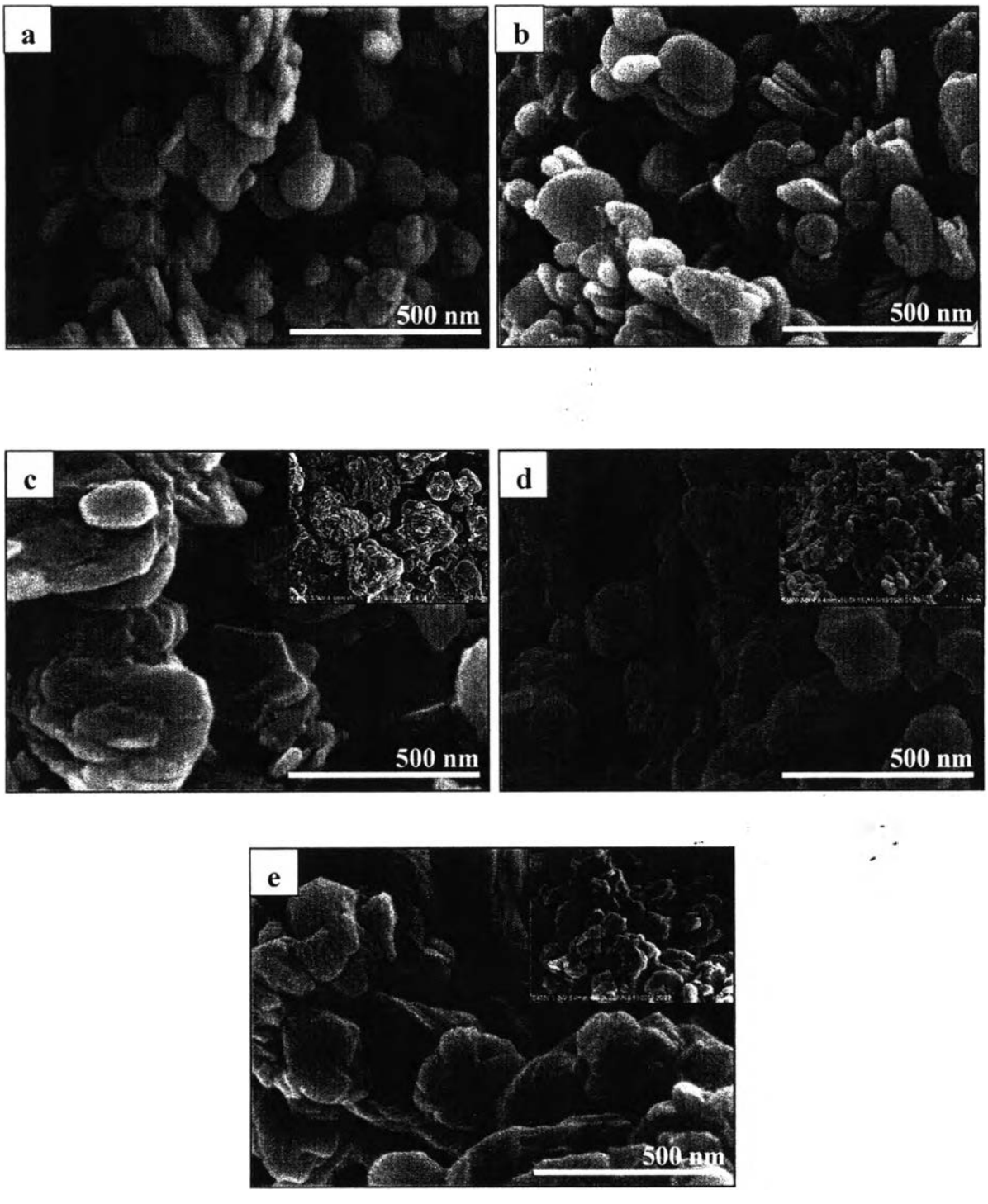

Figure 7.4 SEM micrographs of (a) LDH-CO_3, (b) LDH-NO_3, (c) LDH-C8, (d) LDH-C12, and (e) LDH-C20 at low and high magnifications.

The successful intercalation of these surfactants into LDH layers was eventually confirmed by FTIR spectra (Figure 7.5). The organomodified LDHs show the clear absorption peaks at 1220 and 1065 cm^{-1}, corresponding to symmetric and asymmetric vibration of S=O of the sulfate group and other absorption peaks at 2850–2965 cm^{-1} due to the $-CH_2$ stretching of the hydrocarbon chains. The appearance of the broad characteristic peaks for CO_3^{2-} ions at 1370 (ν_3), 820 (ν_2) and 680 cm^{-1} (ν_4), suggests the remaining of some CO_3^{2-} ions between the layers in agreement with XRD result. The absence both ν_3 peak splitting and ν_1 peak near 1050 cm^{-1} also indicates that the CO_3^{2-} ions lied in a symmetrical site between adjacent metal hydroxide layers (Fuda *et al.* 1993). The presence of interlayer water molecules for the organomodified LDHs samples was indicated by the shoulder absorption peak at 1632 cm^{-1} due to the blending vibration of interlayer H_2O. Therefore, the water molecules present in the organomodified LDHs seem do not interact with the carbonate ions, in stead they located between the hydrocarbon chain end of the surfactants and the metal hydroxide layers as consistent with the result obtained from XRD. Moreover, it should be note that the samples for FTIR measurements were washed several times before use. The fact that the organomodified LDHs still maintain the characteristic absorption peaks related to anionic surfactants. It is demonstrates that the organic guests were strongly adsorbed on the surface of LDHs. As a consequence, the interaction and compatibility between LDH particles and polymer matrix could be greatly improved, which is helpful for the latter preparation of LDPE nanocomposites.

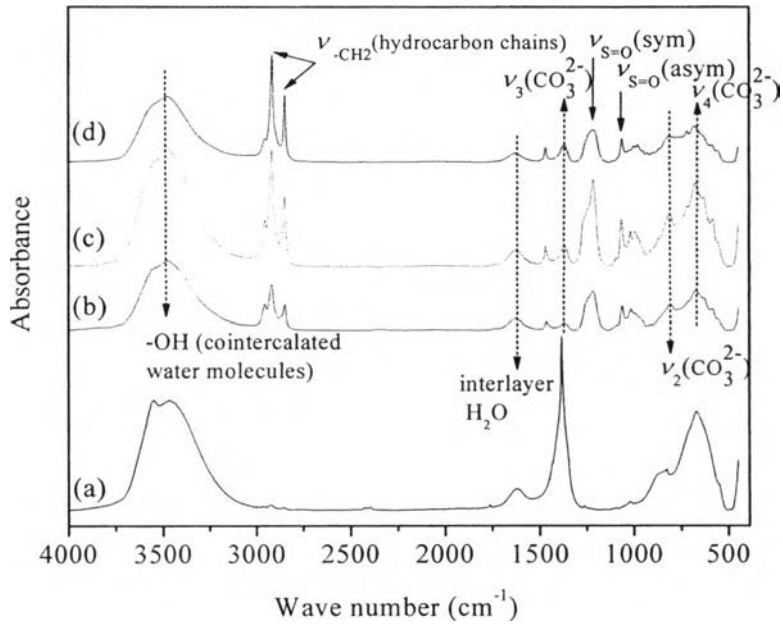

Figure 7.5 The FTIR spectra of (a) LDH-NO_3, (b) LDH-C8, (c) LDH-C12, and (d) LDH-C20.

The TGA/DTG curves of the LDH-NO_3 and the organomodified LDHs are illustrated in Figure 7.6. It can be seen that the LDH-NO_3 exhibits a two steps decomposition process. The first weight loss step, up to 300°C, attributes to the loss of the adsorbed and interlayer water molecules (~9%) and the second weight loss step, between 300–750°C (~37%), corresponds to the loss of the interlayer nitrate and some carbonate ions and the dehydroxylation of the metal hydroxide layers (Kanezaki, 1998). The thermal decomposition behavior of all organomodified LDHs mainly takes place in two steps process. The first decomposition step, up to 180°C (~10%), corresponds to the loss of absorbed water. This step shifts to lower temperatures as compared to the unmodified LDH, which is due to the interaction between interlayer water molecules and the hydroxide layers was much reduced by the incorporation of surfactants molecules (Costa *et al.* 2007). The second decomposition step in the temperature range of 180–800°C (~50%) is due to the degradation of the samples up to the formation of metal oxides. This step and the related exothermic effects involve the overlapping of more processes: the decomposition of intercalated alkyl sulfate surfactants (180–260°C), the loss of some

interlayer carbonate ions interfering with partial dehydroxylation of the layered LDH (260–500°C) and the complete dehydroxylation process of the layered LDH. Among the organomodified LDHs, LDH-C20 exhibits a maximum thermal stability, probably due to the longest hydrocarbon chain that can create much more char and delay the overall thermal decomposition of the layered host. In addition from the thermal analysis also confirms the presence of interlayer water molecules as already discussed by XRD and FTIR.

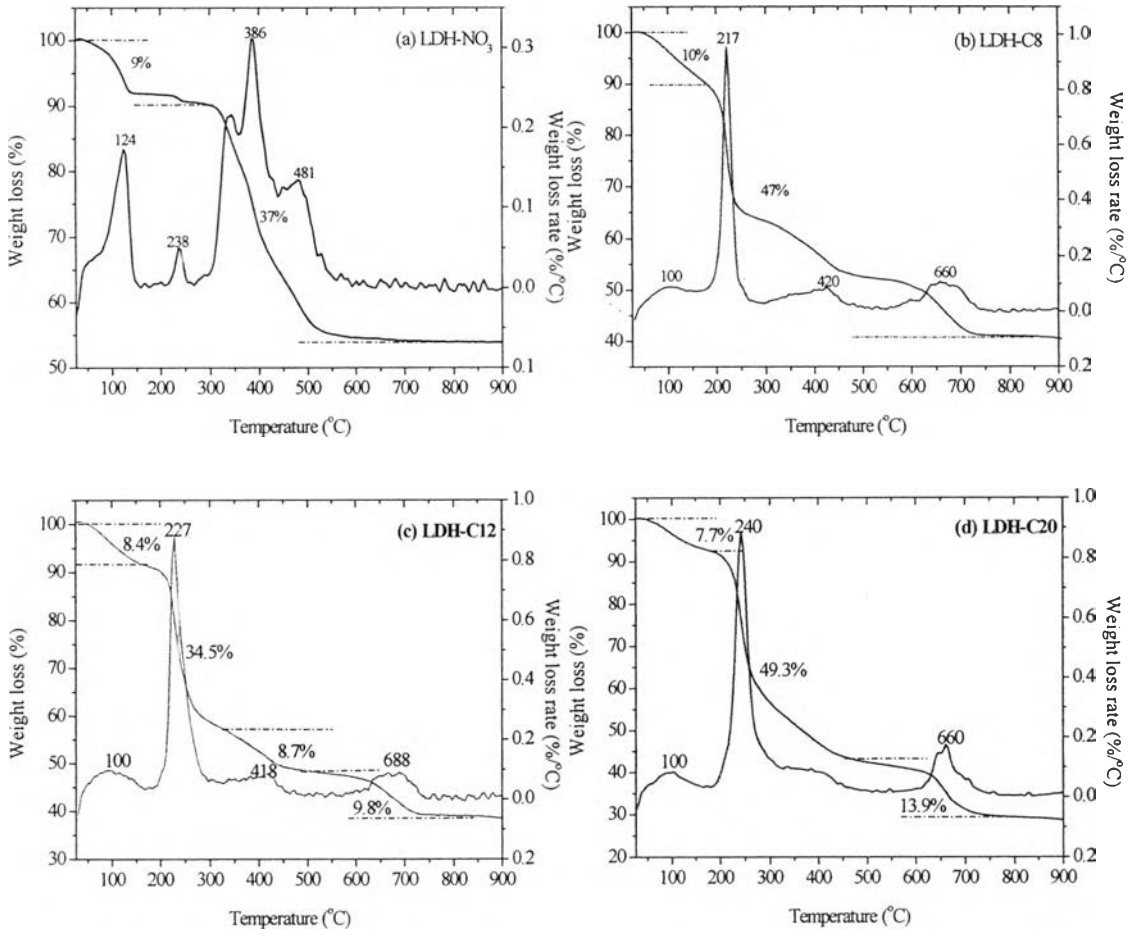

Figure 7.6 TGA/DTG curves of LDH-NO_3 and the organomodified LDHs.

7.3.3 Preparation and Characterizations of LDPE/Organomodified LDHs Nanocomposites

7.3.3.1 Morphological Analysis

LDPE with various organomodified LDHs were prepared in Brabender Plasticoder using melt intercalation method, the amount of clay was fixed at 2.5 wt% for LDH-C8 and LDH-C12 and 1.5 wt% for LDH-C20 (Table 7.2). The PE-g-MAH was used as a compatibilizer with the same amount of the organomodified LDHs added. The torque versus time plot during high temperature melt mixing for all samples is shown in Figure 7.7(a). It is clear that after the addition of organomodified LDH in the molten matrix, no significant change of torque is observed. Usually, the addition of hard particles into molten polymer not only enhances the modulus but also increases the torque of that system. Contrary with our case, the torque seems constant which may come from the plasticizing effect of the surfactants used in this system.

The XRD patterns in the range of 2θ = 1.5–10° for nanocomposites are shown in Figure 7.7(b). In case of LDPE/LDH-C8, the strong (003) basal reflection is observed as well-defined peak at 2θ = 3.9° (2.3 nm), suggesting an ordered intercalated and flocculated morphology were formed. For LDPE/LDH-C12 and LDPE/LDH-C20, a smaller (003) basal reflection is observed at 2θ = 3.18° (2.8 nm) and 2θ = 2.28° (3.9 nm), respectively. For these two samples, we can conclude that the polymer chains were intercalated and the coherent ordered structure of LDH layers is much lower than that of LDPE/LDH-C8, suggesting partially exfoliated/intercalated mixed morphology. Despite the obtained nanocomposites shows slightly increase of d_{003} compared to their pristine organomodified LDHs (Figure 7.3(a)); one interested observation should be noted that the intensity due to their higher order basal reflections, i.e. <006>, <009> distinctly reduced or disappeared. This demonstrates the ordered structure of the metal hydroxide layers in the nanocomposites was destroyed by the intercalated polymer segments (Vaia and Liu, 2002).

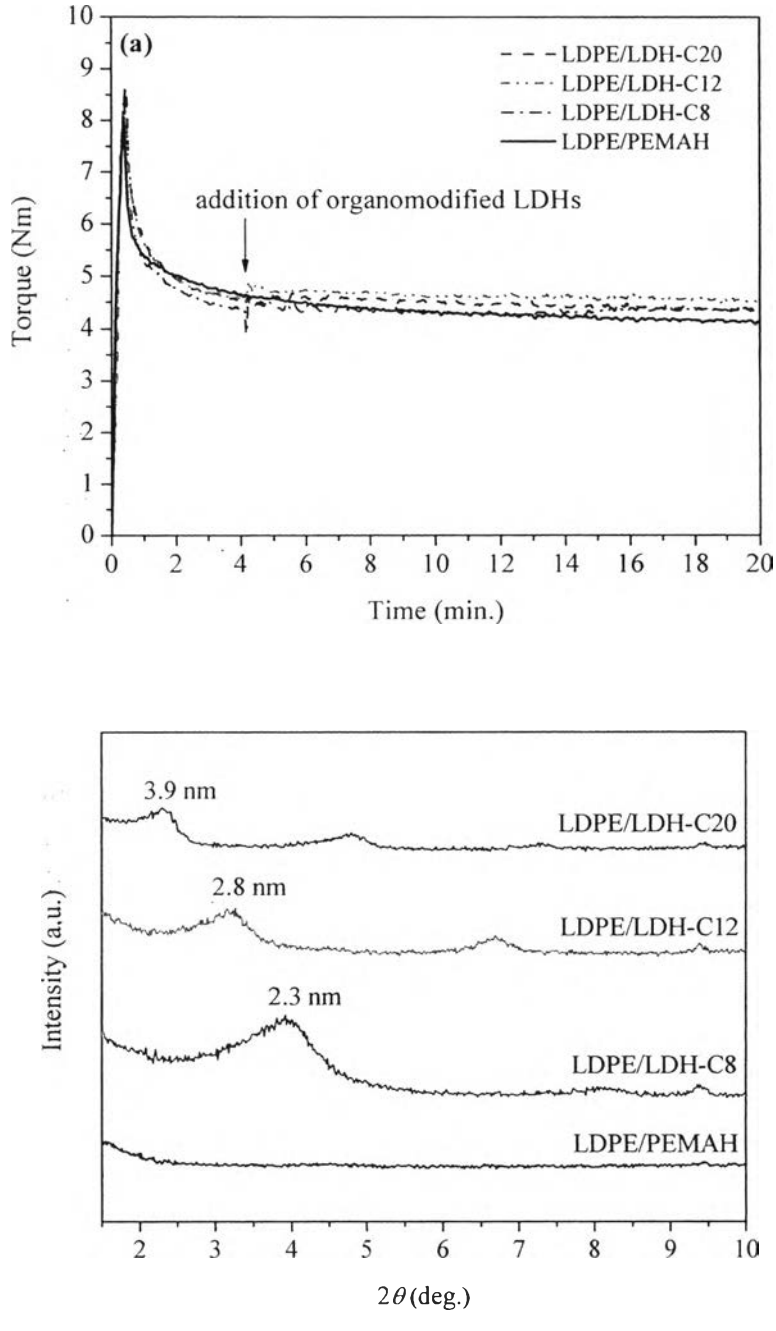

Figure 7.7 Torque vs. time plot during melt mixing (a) and XRD patterns (b) of LDPE/organomodified LDHs nanocomposites.

According to the XRD analysis reveals the mixed morphology of partially exfoliated and intercalated structure for these nanocomposites. To have a clear overview of how dispersion and how orientation of LDH platelets, SEM images at low to high magnification in which being a good representing surface of the bulk polymer matrix, are taking in an account as shown in Figure 7.8(a)–7.8(d) obtained of the fractured surface nanocomposite samples. Apparent for LDPE/LDH-C8 (Figure 7.8(a)) nanocomposite, the LDH-C8 platelets are mainly dispersed in the polymer matrix into two forms: delaminated platelets with the thickness and lateral size of 100–200 nm and 2–3 μm, respectively and aggregated platelets with the thickness and length of 300–600 nm and 2–3 μm, respectively. These aggregates correlated with the strong reflection peak as shown by XRD, can be ascribed to the strong interaction between LDH layers that polymer chains could not separated them apart. On the other hand, a well-defined and homogeneous dispersion of either individual or stacked LDH layers is clearly seen in case of nanocomposite containing LDH-C12 (Figure 7.8(b)) and LDH-C20 (Figure 7.8(c)). However, some aggregates with thickness of few hundred nanometer and length of few micron (see high magnification images, as pointed by the arrows), are evident that agreed well with the present of small peaks in the XRD patterns. There seems that the dispersed platelets were coated well in the polyethylene matrix which probably come from the presence of grafted polar groups (MAH) in the PE chain may have promoted the strong interaction with the hydroxide groups of layered LDH. It is clear that the extent of exfoliation and intercalation completely depends not only on the chain length of the anionic modifiers but also the interaction between the alkyl chains of anionic modifiers and the LDH layers. Either exfoliated or highly intercalated structure is preferable when the number of alkyl chain length is larger ($\geq$ 12).

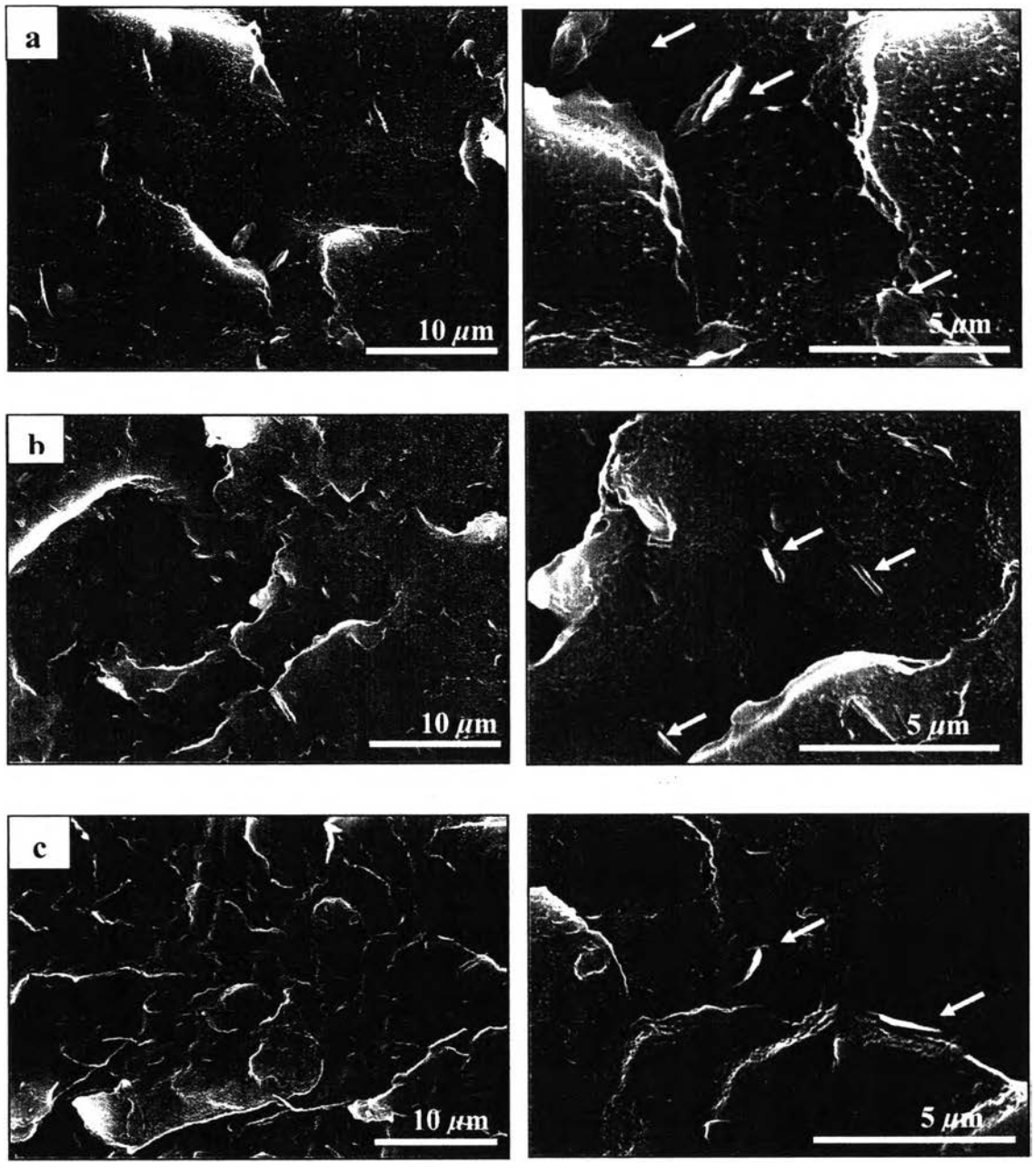

Figure 7.8 SEM micrographs of the nanocomposites (a) LDPE/LDH-C8, (b) LDPE/LDH-C12, and (c) LDPE/LDH-C20 at the low (3000X, left) and high (10000X, right) magnifications.

7.3.3.2 Thermal Analysis

The TGA curves of pure LDPE, LDPE/PEMAH, and the nanocomposites are shown in Figure 7.9(a). The temperature corresponding to 10% and 50% of weight loss ($T_{10\%}$ and $T_{50\%}$), the temperature at maximum rate of weight loss (T_{max}), and the char residue obtained at 900°C are reported in Table 7.2. Two-step decomposition is apparent for the nanocomposites: the first step, temperature range of 200–405°C (~25% weight loss), involves the dehydration of metal hydroxide layers, thermal degradation of the organic modifiers, and the volatilization of the thermo-oxidative product of LDPE (Chen *et al.* 2004); the second step, temperature range of 405–600°C (~15% weight loss), is ascribed to the decomposition of polyethylene chains and volatilization of the residual polymer. In particular, an efficient charring process in flame retardant polymeric materials occurs at a temperature higher than their processing temperature but much lower than their decomposition temperature. It is observed that the initial degradation, i.e. at 10% weight loss for the nanocomposites is faster compared to the pure matrix, which is due to the earlier degradation of the organic modifiers (Qiu, 2006 and Du. 2006). The charred layers produced by the fast degradation of these modifiers, are very advantageous for promoting the charring process, thus enhancing the thermal stability of the polymeric materials. This remarkable enchantment of the thermal properties of the nanocomposites is characterized by a shift of TGA and DTG (see Figure 7.9(b)) curves toward higher temperatures after 25% weight loss or temperature above 400°C. The temperature at maximum rate of weight loss (T_{max}), as shown in Table 7.2, is about 20–33°C higher than the pure matrix. It is observed among these nanocomposites that LDPE/LDH-C8 has the highest degradation temperature even though its microstructure analysis indicated the lowest degree of exfoliation/intercalation. This is probably due to larger aggregates have more area to shield on the surface of the material (Costa *et al.* 2007). It is noteworthy that the degradation temperature of LDPE/LDH-C20 is nearly the same as that of LDPE/LDH-C8 even lower amount of clay was added (1.5 wt%). This infers to the fact that the well-dispersed LDH platelets in the bulk polymer promote the charring process and enhance the flame retardant properties of the polymeric materials. A

similar weight loss behavior has been reported both layered LDH and layered silicate systems (Costa, 2007; Du, 2006; Tang, 2003).

The DSC analysis of the nanocomposites and the corresponding pure matrix was carried out. The melting (T_m) and crystallization (T_c) peak temperatures, as well as the melting enthalpy (ΔH_m) and degree of crystallinity (χ_c), calculated from the second heating run, are summarized in Table 7.2. Most of the nanocomposites show an increase of T_c, especially in the case of LDPE/LDH-C20 but slight decrease of T_m with respected to LDPE/PEMAH blend. The increase in T_c probably concerning with the heterogeneous nucleation activity of the dispersed LDH platelets, just small amount of LDH platelets added could accelerate the crystallization process of LDPE. However, the degree of crystallinity seems unchanged and independent on the types of nanocomposite.

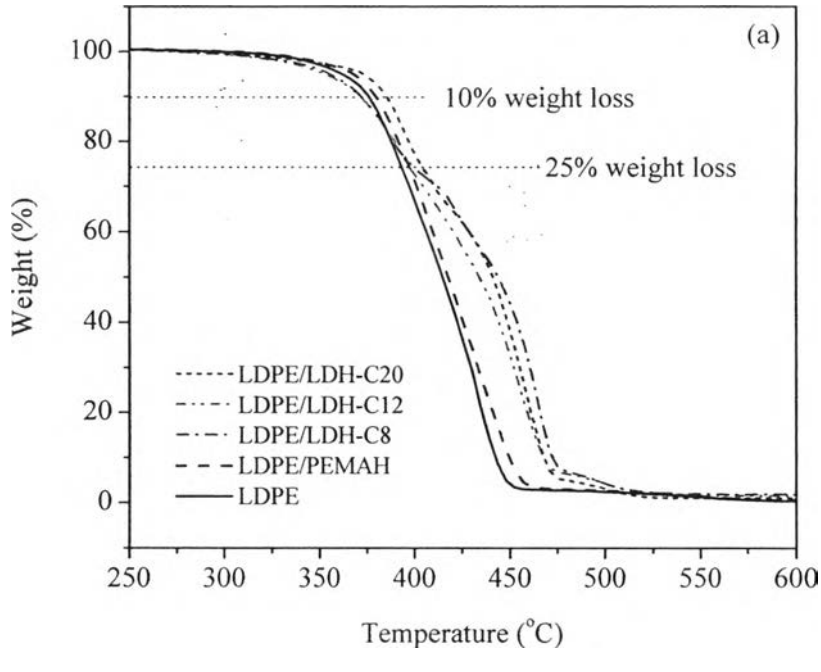

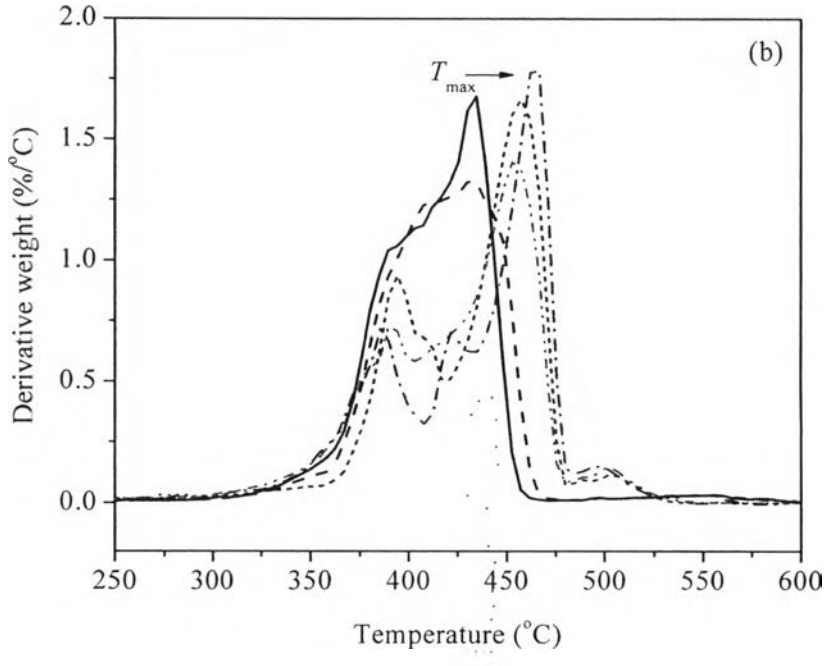

Figure 7.9 TGA (a) and DTG (b) thermograms of LDPE/organomodified LDHs nanocomposites.

E/PEMAH (97.5/2.5)	380.0	431.5	-	84.9	112.3	130.5	44.5	0.48
E/LDH-C8 (97.5/2.5/2.5)	371.8	464.2	32.7	86.4	110.3	126.1	44.1	1.35
E/LDH-C12 (97.5/2.5/2.5)	370.7	452.1	20.6	84.4	112.2	125.6	44.0	1.09
E/LDH-C20 (98.5/1.5/1.5)	384.9	456.8	25.3	86.9	109.6	130.7	45.3	0.68
E/LDH-C12(5wt%) (95/5/5)	367.8	457.0	25.5	84.5	110.0	119.7	43.0	2.13

culated as follow: $\chi_c=\Delta H_m/(1\text{-}x)\Delta H_m^0$, where ΔH_m is the experimental melting enthalpy, *(1-x)* is the polyethylene fraction veight in the composite and ΔH_m^0 is the melting enthalpy of infinite polyethylene crystal (293 J/g).

r residue at 900 °C obtained from TGA analysis.

7.3.3.3 Dynamic Mechanical Properties

The temperature dependences of storage modulus (E'), loss modulus (E''), and loss tangent (tanδ) for the nanocomposites containing different organomodified LDHs are shown in Figure 7.10(a)–(c). Generally, LDPE exhibits three relaxations known as α, β, and γ, are associated with chain motions in crystalline phase, chain motions in amorphous phase, and the motion of three to five of CH_2 chain segments, respectively (Hoffman *et al.* 1996). It can be observed from Figure 7.10(a) that the E' of all samples decreases slowly until –50°C. Subsequently, a very sharp drop appears, related to the β relaxation process, which is predominant in our case and has the properties of glass-rubber transition. The E' of nanocomposites is higher than that of LDPE/PEMAH at the low temperature region (Table 7.3), suggesting the addition of LDH platelets into the polymer increases the stiffness of the final composites. This effect is more noticeable for the composite containing LDH-C8. The increase of E' may contribute in either of two ways: (i) the good dispersion of LDH platelets in the polymer matrix and (ii) the physical crosslinking effect induced by the strong interactions between the polymer and the layered clay (Xie *et al.* 2006).

As mention above, the β relaxation could be assumed as glass transition temperature (T_g) of the composites. It appears from Figure 7.10(b)–7.10(c) that the peak position related to the β relaxation for the nanocomposites shifts to higher temperatures. The significant increase of β relaxation peak temperature or T_g of the nanocomposites may be explained by the stronger interactions between the polymer and layered clay restricted the mobility of the polymer chains. In addition from Figure 7.10(c), the tanδ curves of nanocomposites after room temperature seem to move to higher temperature, which is correlated to α relaxation region. This may suggest that the dispersed clay not only restricted the molecular motion in amorphous phase but also confined the segmental relaxation in the crystalline phase (Hoffman *et al.* 1996). Similar behavior was observed on other system such as EVA/EPDM/ DS-LDH nanocomposite (Kuila *et al.* 2009) and PBT nanocomposite (Berti *et al.* 2009).

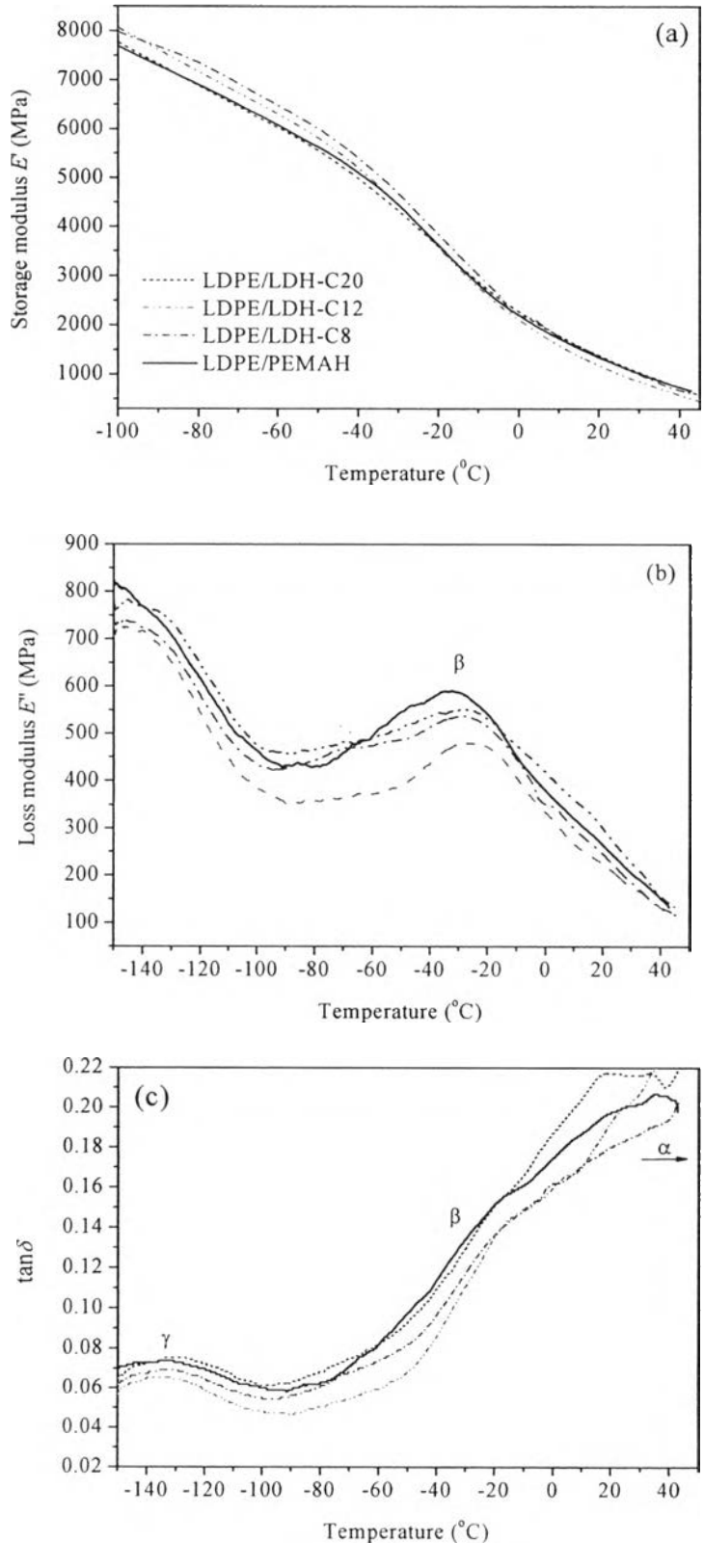

Figure 7.10 The dynamic (a) storage modulus, (b) loss modulus, and (c) loss tangent of LDPE/organomodified LDHs nanocomposites.

Table 7.3 Dynamic storage moduli and peak temperature of relaxations for LDPE/organomodified LDHs nanocomposites

Composites	Storage modulus, E', (MPa)			Relaxations peak temperature, (°C)	
	-100 °C	-80 °C	-60 °C	$\beta(T_g)$	γ
LDPE/PEMAH	7704.8	6911.1	6108.8	-33.6	-133.5
LDPE/LDH-C8 (2.5wt%)	7997.7	7353.6	6479.8	-27.6	-132.2
LDPE/LDH-C12 (2.5wt%)	8075.8	7163.6	6304.1	-25.6	-133.0
LDPE/LDH-C20 (1.5wt%)	7782.9	6911.1	6030.8	-27.1	-129.2
LDPE/LDH-C12 (5.0wt%)	8238.9	7477.6	6712.0	-27.8	-132.0

7.3.3.4 Effect of Organomodified LDH Concentration

Generally, improved or depressed in some particular properties, is usually observed when the amount of the organoclay was increased. For this regarded, the LDH modified with C12 was selected for further preparing LDPE nanocomposites with 5wt%. It can be seen that 5wt% LDH-C12 nanocomposite reveals only broad diffraction peak at $2\theta = 3.4°$ ($d_{003} = 2.7$ nm) where the position closed to the pristine LDH-C12 one, as shown in Figure 7.11(a). This may due to the presence of unintercalated/ of LDH-C12 platelets. Moreover, no peak at lower angles ($2\theta \leq 3$ deg.) is observed, suggesting to existence of exfoliated LDH platelets. Therefore, it can be concluded that 5wt% LDH-C12 nanocomposite establish the exfoliated/intercalated mixed structure. This assumption is confirmed by the SEM micro-analysis at low and high magnification images (Figure 7.11(b)). A good dispersion of LDH platelets is clearly seen trough the matrix polymer. Unfortunately, large interconnection/clustering of several LDH platelet, particle size about 2 μm, is obviously seen relating to the observed in XRD. There seems that this big particles formed by the strong face–face interactions between the adjacent groups (indicated by circle) of either LDH platelets or perhaps individual layers.

In deed, the 5 wt% nanocomposite reveals somewhat improve in the thermal properties such as the increasing of degradation temperature (T_{max}), which is about 5°C higher than the 2.5 wt% one and about 26°C higher than that of pure matrix. The crystallization and melting behaviour seem no significant influenced by the amount of organomodified LDH added (see Table 7.2). A slight decrease of degree of crystallinity (χ_c, presented in Table 7.2) is observed, which probably due to the suppression effect of the aggregated-LDH hindering the growth of crystallite LDPE.

The increase of LDH concentration in the nanocomposite leads to the higher value of the E' through the studied temperature ranges (see Table 7.3), suggesting the addition of the clay enhanced the stiffness of the composite. The temperature dependences of storage modulus enhancement factor, defined as $E'_{real} = E'_{composite}/E'_{pure\ matrix}$ for 2.5 wt% and 5.0 wt% loading of LDH-C12, are presented in Figure 7.11(c). As can be seen, with increasing amount of LDH-C12, the relative storage modulus is increased. This may contribute to the fact that some volume of the composite is occupied by LDH particles, in which storage modulus is much greater than the pure polymer or the lower loading one. There appear two distinct peaks at –46°C and 33°C of 5wt% loading relative modulus curve, which related to the setting up of the chains motion in the amorphous (β relaxation) and the crystalline (α relaxation) phases of the polymer, respectively. While for 2.5wt% loading sample, the relative modulus curve shows nearly constant from the beginning till –10°C, and after suddenly drops. The observed glass transition temperature (T_g) of 5wt% sample slightly decrease compared to 2.5wt% one but much higher than the pure matrix (see Table 7.3).

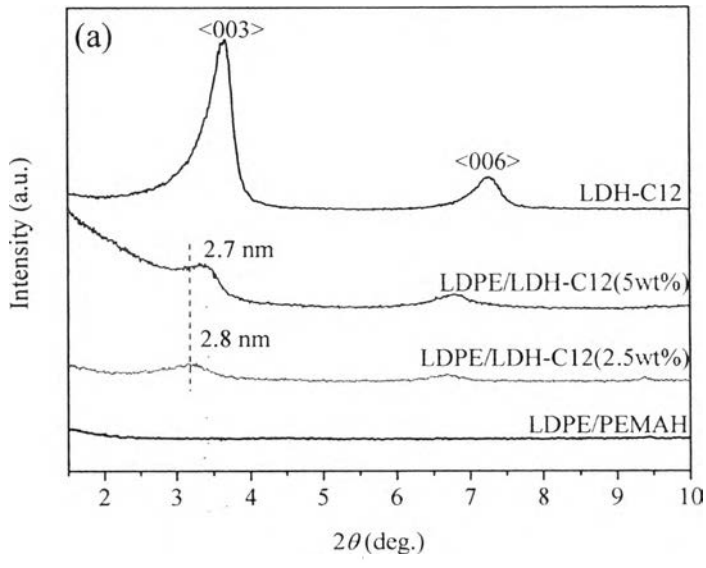
(a)
<003>
<006>
LDH-C12
2.7 nm
LDPE/LDH-C12(5wt%)
2.8 nm
LDPE/LDH-C12(2.5wt%)
LDPE/PEMAH
Intensity (a.u.)
2
3
4
5
6
7
8
9
10
2θ (deg.)

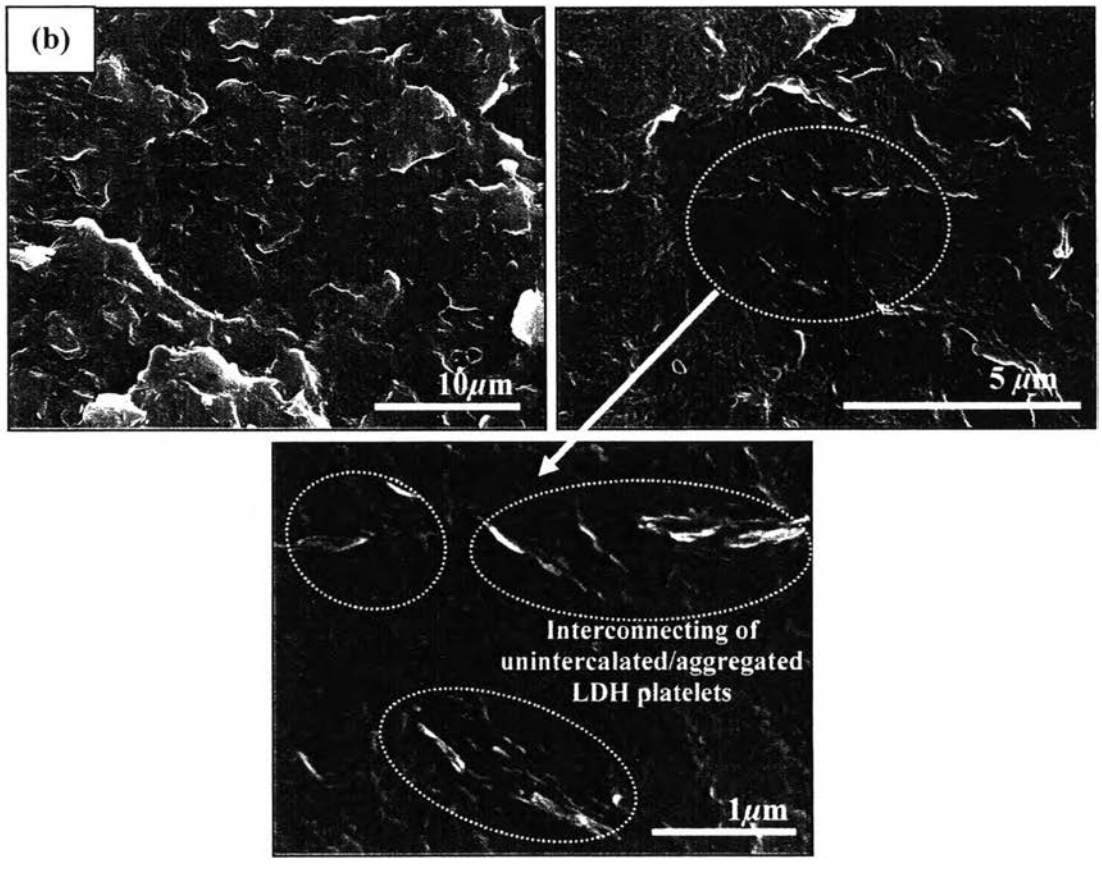
(b)
10μm
5μm
Interconnecting of
unintercalated/aggregated
LDH platelets
1μm

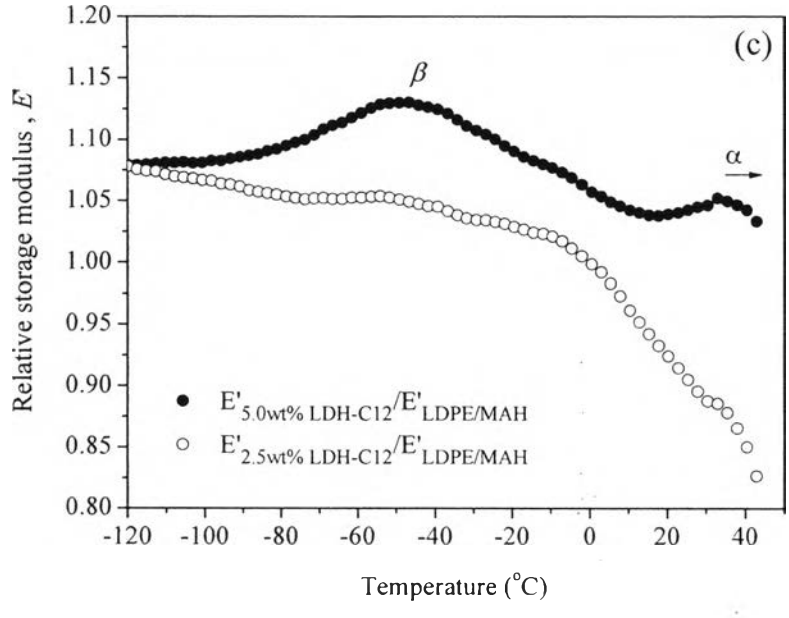

Figure 7.11 (a) compared XRD patterns, (b) low and high magnification SEM images, and (c) temperature dependence of relative storage modulus ($E'_{composite}/E'_{pure\ matrix}$) for 2.5 wt% and 5 wt% of LDH-C12 nanocomposites.

7.4 Conclusions

Low density polyethylene/layered double hydroxide (LDH) nanocomposites were prepared via melt-compounding using polyethylene grafted maleic anhydride (PE-g-MAH) as a compatibilizer. The pristine LDH-CO_3 was first converted to LDH-NO_3 for facilitating the intercalation process of polyethylene chains. LDH-NO_3 was modified by different alkyl chain length of sodium sulfates (n_c = 8, 12, and 20) using ion exchange method. The successful intercalation of the anionic surfactants into LDH layers was characterized by X-ray diffraction (XRD), Fourier transform infrared (FTIR), scanning electron microscopy (SEM), and thermogravimetry (TGA). It was observed that the size of the anionic surfactants played a vital role for the difference in morphological and thermal properties. The obtained nonocomposites established partially exfoliated/intercalated mixed morphology. It was found that the extent of exfoliation and intercalation completely depends not only on the chain length of the anionic modifiers used but also the interaction

between the alkyl chains of anionic modifiers and the LDH layers. Either exfoliated or highly intercalated structure is preferable when the number of alkyl chain length is larger ($\geq$ 12). The TGA analysis showed that LDPE/organomodified LDHs composites exhibited a remarkable enchantment of the thermal properties, in which the decomposition temperature of the nanocomposites is 20–33°C higher than the pure matrix. The DSC results showed the increasing of crystallization temperature. Neither significant change of melting temperature nor degree of crystallinity was observed. The addition of LDH platelets into the polymer enhances the storage modulus of the nanocomposites, which is more noticeable for the composite containing LDH-C8. This increase seems to be influenced by the good dispersion of LDH platelets and the physical crosslinking effect induced by the strong interactions between the polymer and the layered clay. The significant increase of β relaxation peak temperature related to the glass transition temperature (T_g) of the nanocomposites may be explained by the stronger interactions between the polymer and layered clay restricted the mobility of the polymer chains. The effect of the organomodified clay concentration was studied on some properties. It was found that with increasing the concentration, the morphological structure seems no changed but larger of the aggregation/clustering of LDH platelets were evident. In addition, the thermal properties and the storage modulus were significant enhanced.